Characterizing SEU Cross Sections of 12- and 28-nm SRAMs for 6.0, 8.0, and 14.8 MeV Neutrons

Kazusa Takami[1] Yuibi Gomi[1] Shin-ichiro Abe[2] Wang Liao[3]
Seiya Manabe[4] Tetsuro Matsumoto[4] Masanori Hashimoto[1]
[1]Dept. Communications and Computer Engineering, Kyoto University
[2]Nuclear Science and Engineering Center, Japan Atomic Energy Agency
[3]Photon Science Center, University of Tokyo
[4]National Metrology Institute of Japan, National Institute of Advanced Industrial Science and Technology (AIST)

***Abstract*—This paper studies the characteristics of the single event upset (SEU) cross sections in 12- and 28-nm SRAMs induced by low-energy neutrons. Experimental results show that the SEU event cross sections of the 12-nm FinFET SRAM and 28-nm planar SRAM drop less significantly from 14.8 MeV to 6.0 MeV compared with 65-nm SRAM. This result shows that the importance of neutrons below 10 MeV elevates for terrestrial SER estimation for advanced SRAMs.**

I. Introduction

Soft errors caused by terrestrial neutrons have been a severe concern in high-performance computing systems. Although soft errors can be corrected by rebooting, errors on an autonomous driving car or a nursing-care robot could be mortal since abnormal behaviors before rebooting, and no response during rebooting may result in a catastrophic failure. In addition, errors on systems that are expensive and difficult to maintain, such as an artificial satellite, damage economically.

The procedure to characterize soft error rate (SER) in the terrestrial environment is standardized by JEDEC and other groups. According to the test standard of JESD89 [1], neutrons with energies higher than 10 MeV are considered for calculating SER. However, neutrons whose energies are below 10 MeV exist in the terrestrial environment. H. Quinn et al. discuss the impact of <10-MeV neutrons in [2]. References [3]–[5] experimentally pointed out the importance of <10-MeV neutrons with 65-nm SRAM clearly. M. Cecchetto et al. report that 40- and 65-nm SRAMs are more sensitive to <10-MeV neutrons than 90-nm SRAM, and <10-MeV neutrons have more contributions to the estimated SER on 40- and 65-nm SRAMs compared to 90-nm SRAM [6].

When estimating the terrestrial SER with an accelerator, we obtain it by dividing the SER in the test environment by the accelerating factor. However, beam facilities whose neutron spectra are similar to the terrestrial spectrum are only a few worldwide. Therefore, we may use facilities with spallation neutron beams whose energy spectra are somewhat similar to the terrestrial spectrum. In this case, the spectrum difference between the terrestrial and test environments causes concern about the accuracy of the calculated SER.

This work investigates the SEU cross sections of 12-nm FinFET and 28-nm planar SRAMs at 6.0, 8.0, and 14.8 MeV to clarify the importance of <10-MeV neutrons to SER estimation in advanced technologies beyond the 65-nm process. Based on the experimental results, we calculate the estimated SERs in some facilities and discuss the difference between the terrestrial and estimated SERs.

II. Irradiation setup

We used 12-nm FinFET SRAM chips and 28-nm planar SRAM chips for neutron irradiation experiments. Each 12-nm chip includes four types of SRAM macros with different cell areas and the same capacity of 7.08 Mbit. The 12-nm chip includes 28.3 Mbit in total. As for the 28-nm chips, there are two types of memories, SRAM and register file (RF), and they have 14.2 Mbit and 4.72 Mbit, respectively. Overall, the 28-nm chip has 18.9 Mbit. 36 SRAM chips are mounted on a DUT board. Then, the 12- and 28-nm DUT boards have 1019 Mbit and 680 Mbit, respectively.

For characterizing SEUs induced by low-energy neutrons in the SRAM, we used neutron sources at the national metrology institute of Japan (NMIJ) in Advanced Industrial Science and Technology (AIST). NMIJ provides all-direction beams of 6.0, 8.0, and 14.8 MeV. We placed the DUT boards at 10 cm from the beam target to obtain larger fluence, as shown in Fig. 1. The neutrons were injected from the package sides. We irradiated the front board and the tilt board simultaneously. The neutron energy and flux vary depending on the angle and distance from the target. The energy spectra are found in Fig. 1 in [3]. At 0° (ON-axis) direction, the flux is measured by a thick radiator (TR) detector. Note that only the spectra in the direction along the vertical line, namely 0°, are measured for the beam of each original energy, while the spectra along the tilt directions are calculated ones.

We repeated 30-minute static tests for the 12-nm boards and 15-minute tests for the 28-nm boards. All SRAM cells were written into 1, and the operating voltage was set to 0.68 V for 12-nm boards and 0.75 V for 28-nm boards throughout the experiments. Here, we define two cross sections. The first one is based on the number of error bits, which is hereafter called bit cross section. The second is based on the number of events, called event cross section.

III. Energetic dependence of error cross sections

Fig. 2 shows the experimental results of the bit cross section for neutrons of 3.6, 6.0, 7.0, 8.0, and 14.8 MeV. All results in

978-1-6654-5672-2/23/$31.00 ©2023 IEEE

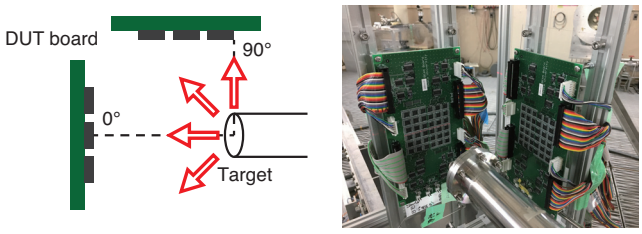

Fig. 1. Irradiation setup.

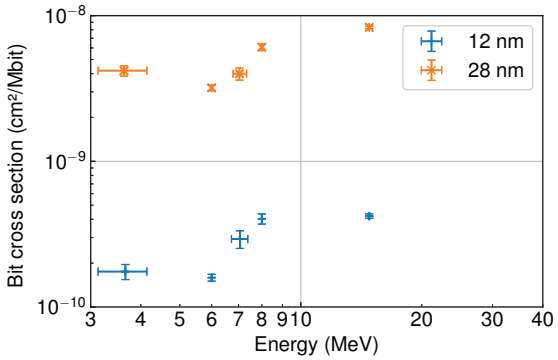

Fig. 2. Energetic dependence of bit cross section. Vertical error bar is with one standard deviation. Horizontal error bar represents the energy spread within one DUT board. In each chip, the memory type difference is not considered.

this paper are illustrated with the error bar of one standard deviation of the number of error bits or events. Here, the memory type difference is not considered, and all bit upsets are equally treated. For the 12-nm SRAM, the minimum and maximum of the bit cross sections are 1.32×10^{-10} cm^2/Mbit at the energy of 6.0 MeV and 4.22×10^{-10} cm^2/Mbit at 14.8 MeV, respectively. As for the 28-nm SRAM, the minimum and maximum are 2.63×10^{-9} cm^2/Mbit at 6.0 MeV and 8.31×10^{-9} cm^2/Mbit at 14.8 MeV, respectively. Comparing the 12-nm and 28-nm SRAMs, the ratio of the 12-nm bit cross section at 6.0 MeV to that at 14.8 MeV is similar to that of the 28-nm SRAM.

Fig. 3 shows the proportion of multiple cell upsets (MCUs) to the total events. The proportion of MCUs on the 12-nm SRAM is less than that on the 28-nm SRAM. Also, we can see the MCU ratio at 6.0 MeV is the smallest, but still, it is 5.6% on the 12-nm SRAM and 17.5% on the 28-nm SRAM.

Fig. 4 shows the bit cross sections by the types of the SRAM macro on the 12-nm SRAM, and Fig. 5 shows those on the 28-nm SRAM. We observe that the bit cross sections vary among the SRAM types on the 12-nm SRAM, where the ratios of the SRAM cell area for type A to D is 1.06, 1.25, 1.00, and 1.31, respectively. Meanwhile, the order of the cross sections differs from the cell area. On the other hand, on the 28-nm SRAM, there is no significant difference at 6.0 and 8.0 MeV, but 27.0% difference exists at 14.8MeV, where the cell area ratio of RF to SRAM is 1.22. In both technologies, further analysis is necessary to explain the difference.

Fig. 6 shows the single bit upset (SBU) and MCU event cross sections on 12-nm, 28-nm, and 65-nm SRAM chips,

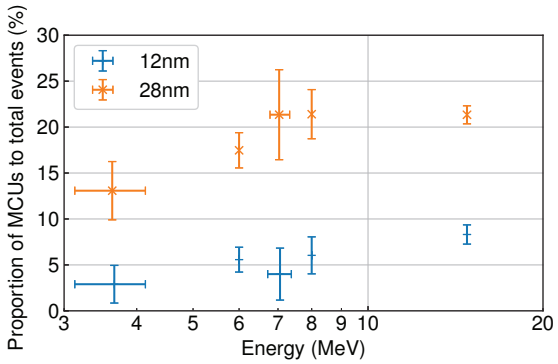

Fig. 3. Proportion of MCUs to total events. Vertical error bar is with one standard deviation. Horizontal error bar represents the energy spread within one DUT board.

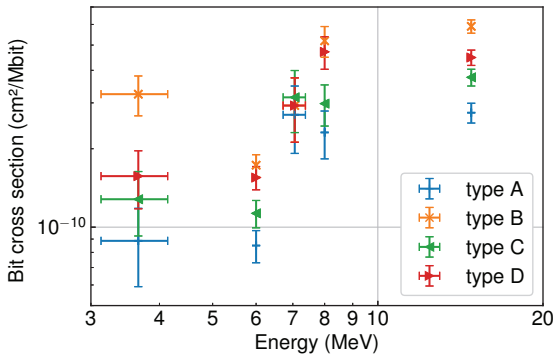

Fig. 4. Energetic dependence of bit cross section of 12-nm SRAM by type. Vertical error bar is with one standard deviation. Horizontal error bar represents the energy spread within one DUT board.

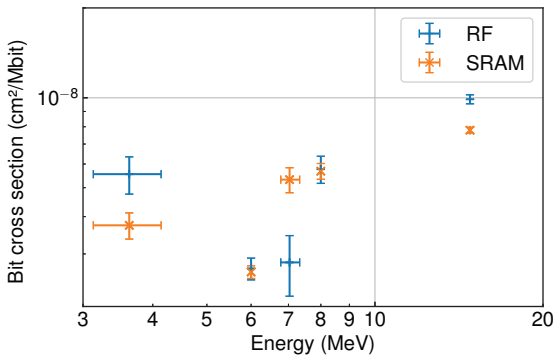

Fig. 5. Energetic dependence of bit cross section of 28-nm SRAM by type. Vertical error bar is with one standard deviation. Horizontal error bar represents the energy spread within one DUT board.

where the 65-nm bulk SRAM data at 1.0 V operation is taken from [3], [5]. Note that the 65-nm SRAM was fabricated with a deep N-well option, and then MCUs tend to occur frequently. Also, the operation voltage of the 65-nm SRAM was 1.0 V. The ratio of the SBU event cross sections of the 12-nm and 28-nm SRAM at 14.8 MeV to that of the 65-nm SRAM are 2.73% and 39.6%, respectively. Also, the ratio of the MCU event cross sections on 12-nm and 28-nm SRAM at 14.8 MeV

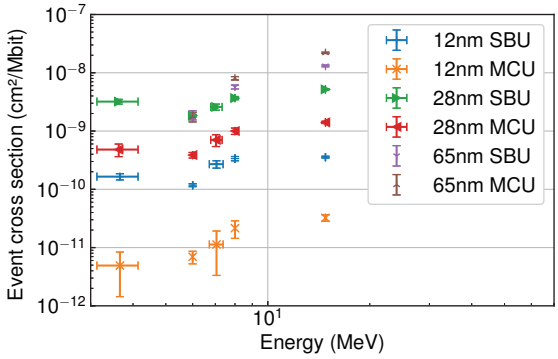

Fig. 6. Energetic dependence of SBU and MCU event cross sections for 12, 28, and 65-nm SRAMs. Vertical error bar is with one standard deviation. Horizontal error bar represents the energy spread within one DUT board.

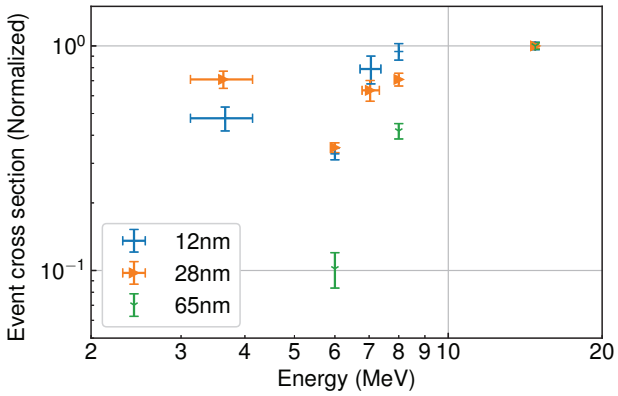

Fig. 7. Energetic dependence of SBUs and MCUs event cross section. For each SRAM, the cross section is normalized by the one at 14.8 MeV. Vertical error bar is with one standard deviation. Horizontal error bar represents the energy spread within one DUT board.

to that on 65-nm SRAM are 0.147% and 6.41%, respectively.

Fig. 7 shows the SEU cross sections of the three technologies, each of which is normalized by the corresponding cross section at 14.8 MeV. We can see that the 12-nm and 28-nm SRAMs have a smaller change in the normalized SEU event cross section from 6.0 MeV to 14.8 MeV than the 65-nm SRAM. The ratio of the normalized SEU cross section for the 12-nm to that for the 65-nm at 6.0 MeV is 3.2. This result indicates that <10 MeV neutrons play a more important role in the SER estimation in the 12-nm and 28-nm SRAMs.

IV. Terrestrial SER Evaluation Based on Measured Energetic Dependence of Cross Sections

A. Contribution of Low-Energy Neutron to Terrestrial SER

Based on the measurement results above, we calculate terrestrial SERs at Tokyo, Japan, and NYC, USA with the differential fluxes of neutrons above 1 MeV calculated by EXPACS [7]. For SER evaluation, we applied the formula below:

$$\mathrm{SER} = \int_{E_0}^{\infty} \sigma(E) \cdot \phi(E) dE, \tag{1}$$

where E represents the energy of neutron, $\sigma(E)$ represents SEU cross section as a function of the neutron energy E, and $\phi(E)$ represents the differential flux as a function of E. E_0 is the cut-off energy for SEU occurrence. Here, we made the following three assumptions for the enegetic dependence which are approximately the same as [3].

1) The cut-off energy for neutrons to induce upset events is 1 MeV. Namely, E_0 is 1 MeV.
2) The cross section keeps the same value from 1 to 6 MeV.
3) The cross section reaches the saturated value above 70 MeV, which is 1.1 times the cross section at 14.8 MeV.

On these assumptions, we use a modified Weibull function below:

$$\sigma(E) = \begin{cases} \sigma_{6\,\mathrm{MeV}}, & (E \le 6\,\mathrm{MeV}) \\ \max\left[\sigma_{6\,\mathrm{MeV}}, A\left\{1 - e^{-\left(\frac{E-E_{\mathrm{onset}}}{w}\right)^S}\right\}\right], & (E > 6\,\mathrm{MeV}) \end{cases} \tag{2}$$

where E_{onset} is supposed to be 6.0 MeV, and A is the saturated value of the cross section. Other parameters in Eq. (2) are determined by the least-squares method with the data of cross sections at 6, 8, and 14.8 MeV. The determined parameters are listed in Table I.

TABLE I
Parameters in Weibull Function in Eq. (2).

Technology	A	$\sigma_{6\,\mathrm{MeV}}$	w	S
12 nm	3.93×10^{-10}	1.18×10^{-10}	0.750	0.683
28 nm	5.71×10^{-9}	1.83×10^{-9}	1.77	0.281
65 nm	3.99×10^{-8}	3.69×10^{-9}	4.68	0.868

The results of SER evaluation on 12-nm, 28-nm SRAM, and 65-nm chips are shown in Fig. 8. The contributions of the neutrons whose energy is 1–10 MeV and above 10 MeV are expressed by different colors. From Fig. 8, we observe that the contributions of the low-energy neutrons to the total SERs on 65-nm SRAM are minor. However, those on 12-nm and 28-nm SRAMs are approaching to 20% and unignorable.

B. Impact of Neutrons below 10 MeV on Accelerating Factor and Estimated Terrestrial SER

Terrestrial SER is often estimated using accelerated irradiation tests with spallation neutron sources, as mentioned in Section I. JESD89 [1] suggests that the low-energy neutrons below 10 MeV should be excluded in calculating the accelerating factor. Here, the accelerating factor is defined as the proportion of the test facility flux to the terrestrial flux because the low-energy neutrons have only a limited impact on the total soft error events. However, the difference in the energy spectrum between the terrestrial and irradiation test environments causes some errors in estimating the SER. In this section, the errors of the estimated SERs are assessed quantitatively.

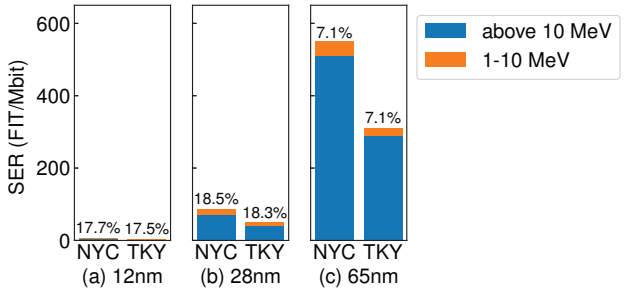

Fig. 8. SERs at NYC and Tokyo. The contributions of neutrons whose energy is 1–10 MeV and above 10 MeV are expressed by different colors. The contribution of neutrons between 1 and 10 MeV is also presented numerically.

This section uses two definitions of SER: terrestrial SER and estimated SER. The former is the SER in NYC mentioned in the previous subsection. The latter is defined as $\mathrm{SER_{est}}$, which is the error rate obtained in the accelerated test $(\mathrm{SER_{facility}})$ divided by accelerating factor $(\mathrm{Acc_{facility}})$:

$$\begin{aligned}\mathrm{SER_{est}} &= \frac{\mathrm{SER_{facility}}}{\mathrm{Acc_{facility}}}, \\ &= \frac{\int_{E_0}^{\infty} \sigma(E) \cdot \phi_{\mathrm{facility}}(E) dE}{\int_{E_{\min}}^{\infty} \phi_{\mathrm{facility}}(E) dE / \int_{E_{\min}}^{\infty} \phi_{\mathrm{NYC}}(E) dE}, \end{aligned} \tag{3}$$

where $\phi_{\mathrm{facility}}(E)$ is the differential neutron flux at the beam facility of interest, and $\phi_{\mathrm{NYC}}(E)$ is the differential neutron flux at NYC. $E_{\min}$ is the lower limit of the integration of each flux. E_0 is equal to 1 MeV, and it is the lower limit of the integration of the product of SEU cross section and the differential neutron flux of the facility. As shown in Eq. (3), the accelerating factor $\mathrm{Acc_{facility}}$ depends on the integration lower limit, $E_{\min}$.

To analyze the dependence of the estimation errors on $E_{\min}$, we calculate the estimated SERs by changing $E_{\min}$ from 1 MeV to 10 MeV by 1 MeV. As representative spallation neutron sources, we choose Los Alamos Neutron Science Center (LANSCE) [8], TRIUMF [9], ChipIr [10], Research Center for Nuclear Physics (RCNP) [11], and BL10 at J-PARC [12]. The proportion of neutrons between 1 and 10 MeV in each facility and NYC and accelerating factors in each facility are shown in Table II. BL10 at J-PARC is chosen because it contains much more low-energy neutrons than the other facilities.

TABLE II
PROPORTION OF NEUTRONS BETWEEN 1 AND 10 MEV IN EACH FACILITY AND ACCELERATING FACTOR.

Facility	% of 1–10 MeV	Accelerating Factor		
		$E_{\min}$ = 1 MeV	$E_{\min}$ = 6 MeV	$E_{\min}$ = 10 MeV
ChipIr	75.7%	4.83×10^9	2.11×10^9	1.86×10^9
BL10	91.9%	1.72×10^9	0.33×10^9	0.22×10^9
LANSCE	54.6%	1.04×10^9	0.82×10^9	0.75×10^9
TRIUMF	29.6%	0.76×10^9	0.83×10^9	0.84×10^9
RCNP	56.5%	0.33×10^9	0.24×10^9	0.23×10^9
NYC (Ref.)	37.0%	-	-	-

Fig. 9 shows the estimated SERs on 12-nm SRAM, and Fig. 10 shows those on 28-nm SRAM. We observe that Fig. 9 and Fig. 10 show a similar tendency. The estimated SERs in ChipIr and BL10 are much higher than those above 3 MeV and lower at 1 MeV. Besides, those in LANSCE and RCNP are higher above 6 MeV and lower at 1 MeV. We observe that the facility with more 1–10 MeV neutrons tends to have larger errors in the estimated SER. Meanwhile, those in TRIUMF do not cause large errors at any $E_{\min}$ values. Fig. 11 shows the estimated SERs on 65-nm SRAM. We can see that their errors are relatively smaller than those on 12- and 28-nm SRAMs at higher $E_{\min}$ and are larger at lower $E_{\min}$.

Fig. 12 shows the sum of the errors between the estimated SERs in each facility and the terrestrial SER. The ordinate of this graph represents the sum of the absolute errors between the estimated SERs and the terrestrial SER with 1 MeV step. The values are normalized by the terrestrial SER on each SRAM. From this figure, we observe that they are minimized when $E_{\min}$ is between 4 and 5 MeV on 65-nm SRAM, whereas $E_{\min}$ is 2 MeV on 12- and 28-nm SRAMs. The relative increase of the cross sections in the low-energy region could lower appropriate $E_{\min}$ to reproduce the terrestrial SER from irradiation experiments with spallation neutron beams.

V. CONCLUSION

This work performed neutron irradiation experiments showing that the cross sections at lower energy below 10 MeV on 12- and 28-nm SRAMs increase relative to those on 65-nm SRAM. We performed the terrestrial SER analysis based on the measured dependence of SEU cross sections on neutron energy. Although the low-energy neutrons from 1 to 10 MeV contribute to the total SER on 65-nm SRAM is only 7%, the contribution on 12- and 28-nm SRAMs is as much as about 18%. In estimating terrestrial SER, the current standard suggests that neutrons below 10 MeV should be excluded in accelerating factor calculation. However, the larger contribution of low-energy neutrons on 12- and 28-nm SRAMs may induce significant errors in the estimated SER. In this case, a lower threshold, which is 2 MeV in this work, is more appropriate for SER estimation.

ACKNOWLEDGEMENT

This work is supported by Socionext Inc. and the Grant-in-Aid for Scientific Research (S) from Japan Society for the Promotion of Science (JSPS) under Grant JP19H05664.

REFERENCES

[1] JEDEC, "Measurement and Reporting of Alpha Particle and Terrestrial Cosmic Ray Induced Soft Error in Semiconductor Devices", JEDEC Standard JESD89B, Sep. 2021.
[2] H. Quinn, et al., "The effect of 1–10-MeV neutrons on the JESD89 test standard," *IEEE TNS*, 66(1), Jan. 2019.
[3] W. Liao, et al., "Characterizing Energetic Dependence of Low-energy Neutron-induced SEU and MCU and Its Influence On Estimation of Terrestrial SER in 65 nm Bulk SRAM," *IEEE TNS*, 68(6), June 2021.
[4] S. Abe, et al., "Impact of Hydrided and Non-Hydrided Materials Near Transistors on Neutron-Induced Single Event Upsets," *Proc IRPS*, 2020.
[5] S. Abe, et al., "A Terrestrial SER Estimation Methodology with Simulation and Single-Source Irradiation Applicable to Diverse Neutron Sources," *Proc. of RADECS*, 2022.

[6] M. Cecchetto et al., "0.1–10 MeV Neutron Soft Error Rate in Accelerator and Atmospheric Environments," *IEEE TNS*, 68(5), May 2021.
[7] T. Sato, "Analytical Model for Estimating the Zenith Angle Dependence of Terrestrial Cosmic Ray Fluxes", PLOS ONE, 11(8), 2016.
[8] P. W. Lisowski and K. F. Schoenberg, "he Los Alamos neutron science center," *Nucl. Instrum. Methods Phys. Res. A, Accel. Spectrom. Detect. Assoc. Equip.,* vol. 562, no. 2, pp. 910–914, Jun. 2006.
[9] E. W. Blackmore, P. E. Dodd, and M. R. Shaneyfelt, "Improved capabilities for proton and neutron irradiations at TRIUMF," in *Proc. IEEE Radiat. Effects Data Workshop*, Jul. 2003, pp. 149–155.
[10] C. Cazzaniga and C. D. Frost, "Progress of the scientific commissioning of a fast neutron beamline for chip irradiation," in *Proc. J. Phys., Conf.,* vol. 1021, May 2018, Art. no. 012037.
[11] Y. Iwamoto *et al.*, "Evaluation of the white neutron beam spectrum for single-event effects testing at the RCNP cyclotron facility," *Nucl. Technol.*, vol. 173, no. 2, pp. 210–217, Feb. 2011.
[12] F. Maekawa *et al.*, "NOBORU: J-PARC BL10 for facility diagnostics and its possible extension to innovative instruments," *Nucl. Instrum. Methods Phys. Res. A, Accel. Spectrom. Detect. Assoc. Equip.,* vol. 600, no. 1, pp. 335–337, Feb. 2009.

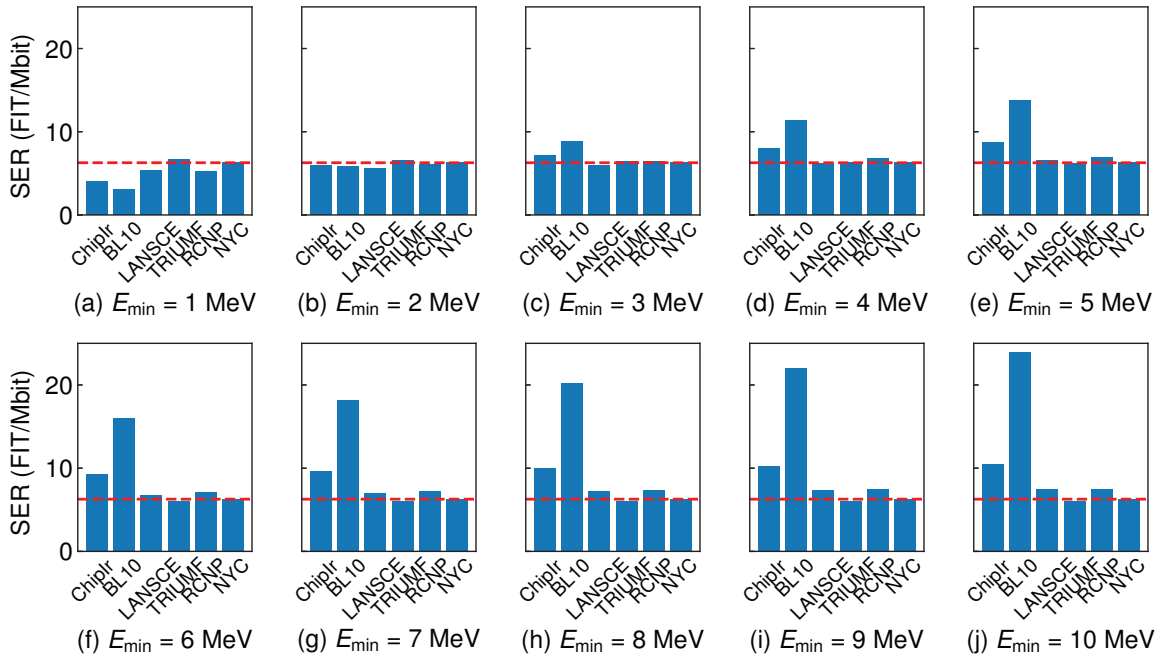

Fig. 9. Estimated SERs on 12-nm SRAM with different E_{min}. In each graph, the terrestrial SER at NYC is added with a horizontal line for comparison.

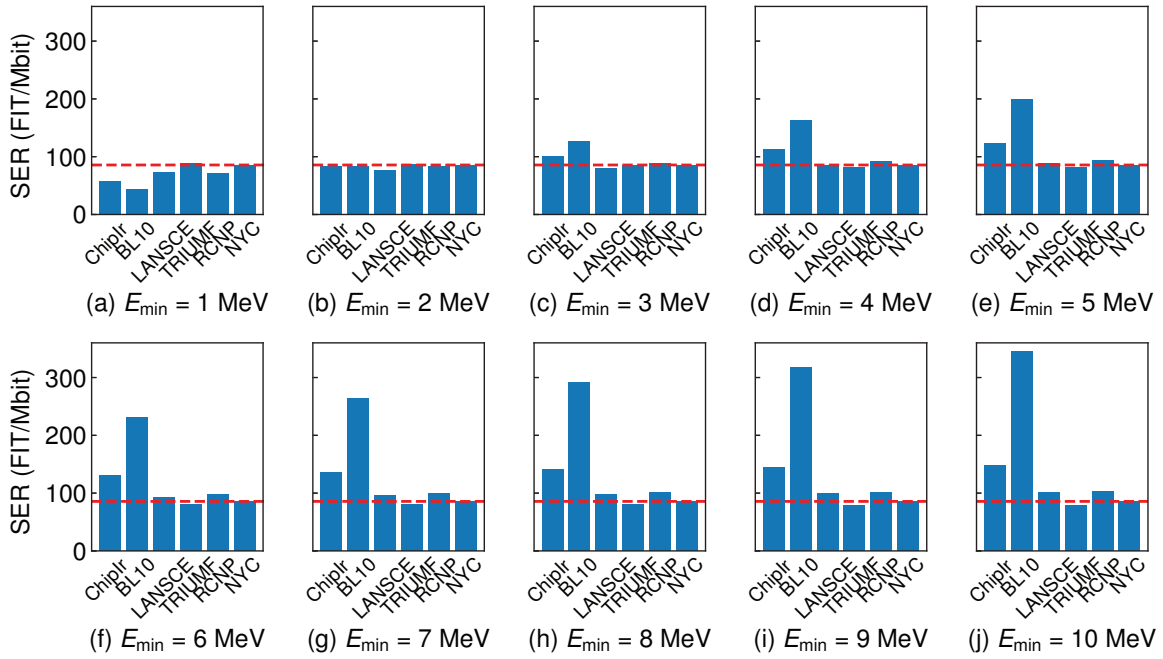

Fig. 10. Estimated SERs on 28-nm SRAM with different E_{min}. In each graph, the terrestrial SER at NYC is added with a horizontal line for comparison.

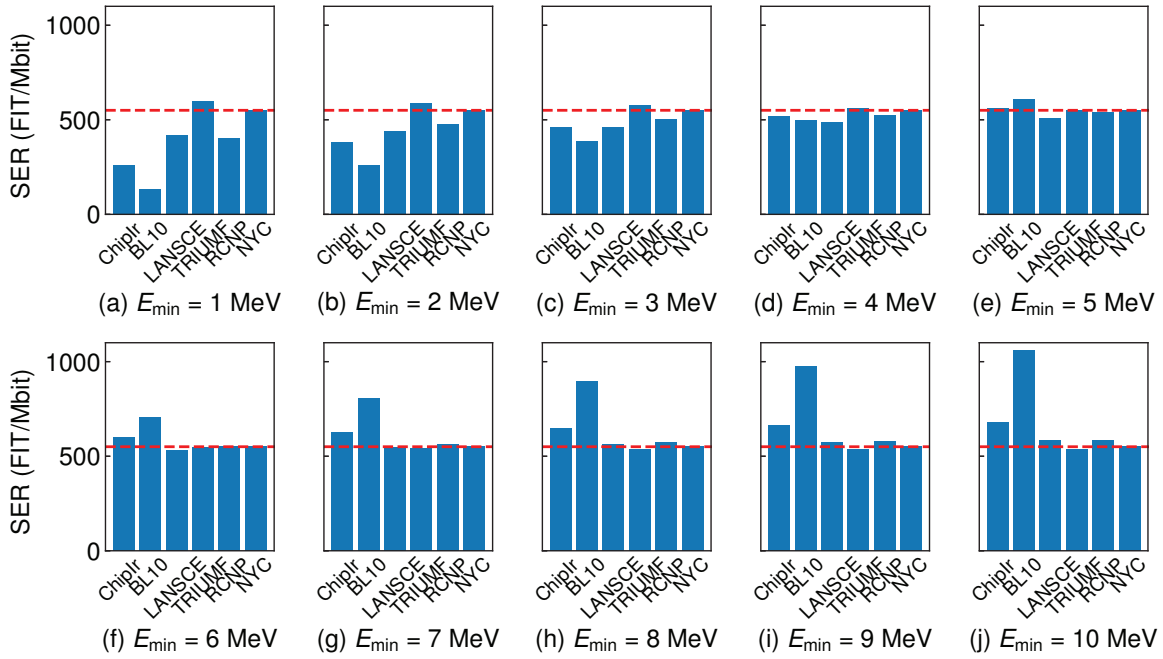

Fig. 11. Estimated SERs on 65-nm SRAM with different $E_{\min}$. In each graph, the terrestrial SER at NYC is added with a horizontal line for comparison.

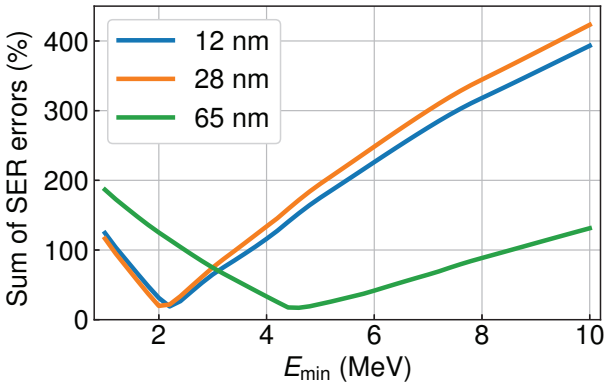

Fig. 12. Relationship between $E_{\min}$ and sum of SER errors. Vertical axis represents the sum of the errors between the estimated SERs in individual facilities and terrestrial SER. The sum of the errors are normalized by terrestrial SER, and the unit of them is %.